

7-2008

Soft and Collinear Enhancements to Top Quark and Higgs Cross Sections

Nikolaos Kidonakis

Kennesaw State University, nkidonak@kennesaw.edu

Follow this and additional works at: <https://digitalcommons.kennesaw.edu/facpubs>



Part of the [Physics Commons](#)

Recommended Citation

Kidonakis N. 2008. Soft and collinear enhancements to top quark and higgs cross sections. *Acta Phys Pol B* 39(7):1593-604.

This Article is brought to you for free and open access by DigitalCommons@Kennesaw State University. It has been accepted for inclusion in Faculty Publications by an authorized administrator of DigitalCommons@Kennesaw State University. For more information, please contact digitalcommons@kennesaw.edu.

SOFT AND COLLINEAR ENHANCEMENTS
TO TOP QUARK AND HIGGS CROSS SECTIONS*

NIKOLAOS KIDONAKIS

Kennesaw State University, Physics #1202
1000 Chastain Rd., Kennesaw, GA 30144-5591, USA*(Received May 6, 2008)*

I present calculations of soft and collinear corrections to the cross-sections for single top quark production, and for Higgs production via $b\bar{b} \rightarrow H$ at the Tevatron and the LHC. I show that the corrections provide significant enhancements to the cross-sections in both cases. For single top production the soft gluon corrections dominate the cross-section, particularly in the s -channel and in tW production. For Higgs production it is shown that purely collinear terms have to be included as well to provide an accurate calculation.

PACS numbers: 12.38.Bx, 12.38.Cy, 14.65.Ha, 14.80.Bn

1. Introduction

The top quark and the Higgs boson are elementary particles that are the epicenter of a lot of theoretical and experimental study due to their significance to electroweak theory and QCD. The importance of these particles to the Standard Model requires that we understand their cross-sections at hadron colliders with the highest achievable accuracy.

The top quark is the heaviest known elementary particle and was discovered in proton-antiproton collisions at the Fermilab Tevatron by the CDF and D0 experiments in 1995 [1, 2]. The discovery of the top quark was through the production of top-antitop pairs. Since then there has been a continuing effort (for a review see [3, 4]) to understand the properties of the top and refine the measurement of the value of its mass. The $t\bar{t}$ cross-section has been calculated to high accuracy by including next-to-next-to-leading-order (NNLO) threshold corrections [5], which dominate the cross-section. The experimental values for the cross-section [6, 7] are in good agreement with the theoretical prediction [5].

* Presented at the Cracow Epiphany Conference on LHC Physics, Cracow, Poland, 4-6 January 2008.

The top quark can also be produced in single top production through t -channel processes involving the exchange of a space-like W boson, s -channel processes involving the exchange of a time-like W boson, and tW production processes involving the production of a W boson in association with the top quark. However, the cross-section is smaller than for $t\bar{t}$ production and the signal is complicated by relatively large backgrounds. Nevertheless, there is now recent evidence of single top production [8, 9]. The interest in this process is due to the fact that it allows a measurement of the V_{tb} CKM matrix element and other electroweak properties of the top quark, and it may play a role in the discovery of new physics.

The search for the Higgs boson [10] is currently the most important goal at the Tevatron and the LHC colliders [11]. In the Standard Model it is expected that the dominant production channel at either collider will be $gg \rightarrow H$. However, the channel $b\bar{b} \rightarrow H$ can also be important in the Minimal Supersymmetric Standard Model at high $\tan\beta$, the ratio of the vacuum expectation values for the two Higgs doublets.

Since both the top quark and the Higgs boson are very massive, their production cross-sections receive large corrections from soft and collinear gluon corrections, which can dominate the cross-section near threshold. These threshold corrections arise from incomplete cancellations of infrared divergences between virtual diagrams and real diagrams with soft (low-energy) gluons. The corrections exponentiate and can thus be resummed.

For single-top production we have processes of the form $p_1 + p_2 \rightarrow p_3 + p_4$, and we define $s = (p_1 + p_2)^2$, $t = (p_1 - p_3)^2$, $u = (p_2 - p_3)^2$ and $s_4 = s + t + u - m_3^2 - m_4^2$. At threshold $s_4 \rightarrow 0$. The soft corrections take the form $[\ln^k(s_4/m_t^2)/s_4]_+$, with m_t the top quark mass and $k \leq 2n - 1$ for the $\mathcal{O}(\alpha_s^n)$ corrections [12]. Near threshold these corrections are dominant and provide excellent approximations to the full cross-section.

For Higgs production, we define $z = m_H^2/s$, where m_H is the Higgs mass, and $z \rightarrow 1$ at threshold. The soft corrections now take the form $[\ln^k(1-z)/(1-z)]_+$ [13, 14]. For $b\bar{b} \rightarrow H$, in addition to the soft corrections, we also have to include purely collinear corrections of the form $\ln^k(1-z)$ in order to achieve a good approximation [14]. The n -th order corrections in the partonic cross-section for $b\bar{b} \rightarrow H$ can be written as

$$\hat{\sigma}^{(n)}(z) = V^{(n)}\delta(1-z) + \sum_{k=0}^{2n-1} S_k^{(n)} \left[\frac{\ln^k(1-z)}{1-z} \right]_+ + \sum_{k=0}^{2n-1} C_k^{(n)} \ln^k(1-z), \quad (1.1)$$

with a similar expression holding for single-top production. The hadronic cross-section, σ , is calculated by integrating the product of the partonic cross-section, $\hat{\sigma}$, and parton distribution functions, ϕ , over the momenta fractions of the protons and/or antiprotons carried by the partons in the hard scattering, at factorization scale μ_F and renormalization scale μ_R :

$$\sigma = \sum_f \int dx_1 dx_2 \phi_{f_1/p}(x_1, \mu_F) \phi_{f_2/\bar{p}}(x_2, \mu_F) \hat{\sigma}(z, \mu_F, \mu_R, \alpha_s). \quad (1.2)$$

2. Resummed cross-section and NNNLO expansions

The resummation of soft and collinear gluon corrections is performed in moment space and it follows from the factorization properties of the cross-section. For the process $b\bar{b} \rightarrow H$ we can write the resummed cross-section as [14–16]

$$\begin{aligned} \hat{\sigma}^{\text{res}}(N) = & \exp[2E_q(N)] \exp[2E_q^{\text{coll}}(N)] \exp\left[4 \int_{\mu_F}^{m_H} \frac{d\mu}{\mu} \gamma_{q/q}(N, \mu)\right] \\ & \times H(\mu_R) S\left(\frac{m_H}{\tilde{N}}\right) \exp\left[\int_{m_H}^{\frac{m_H}{\tilde{N}}} \frac{d\mu}{\mu} 2\text{Re}\Gamma_S(\mu)\right], \end{aligned} \quad (2.1)$$

where

$$\begin{aligned} E_q(N) = & -C_F \int_0^1 dz \frac{z^{N-1} - 1}{1-z} \\ & \times \left\{ \int_{(1-z)^2}^1 \frac{d\lambda}{\lambda} \frac{\alpha_s(\lambda m_H^2)}{\pi} + \frac{\alpha_s((1-z)^2 m_H^2)}{\pi} \right\} + \mathcal{O}(\alpha_s^2), \end{aligned} \quad (2.2)$$

and a somewhat similar expression holds for single top production [12]. Here $C_F = (N_c^2 - 1)/(2N_c)$ with N_c the number of colors. The purely collinear logarithms are resummed in the second exponent, E_q^{coll} , which has a form similar to Eq. (2.2) with the substitution $-(z^{N-1} - 1)/(1-z) \rightarrow z^{N-1}$. The quark anomalous dimensions are denoted by $\gamma_{q/q}$, H is the hard-scattering factor, Γ_S is the soft anomalous dimension which describes the evolution of the soft function S , and $\tilde{N} = Ne^{\gamma_E}$ with γ_E the Euler constant. Inverting Eq. (2.1) back to momentum space, we now provide next-to-next-to-next-to-leading-order (NNNLO) expansions of the resummed cross-section.

At next-to-leading order (NLO) the soft and collinear gluon corrections are

$$\hat{\sigma}^{(1)} = F^{\text{B}} \frac{\alpha_s(\mu_{\text{R}}^2)}{\pi} \left\{ c_3 \left[\frac{\ln(1-z)}{1-z} \right]_+ + c_2 \left[\frac{1}{1-z} \right]_+ + c_1 \delta(1-z) + c_3^c \ln(1-z) + c_2^c \right\}, \quad (2.3)$$

where F^{B} is the Born term. The leading coefficients for $b\bar{b} \rightarrow H$ are $c_3 = 4C_{\text{F}}$, $c_3^c = -4C_{\text{F}}$ and the subleading coefficients are given in [14]. Expressions for all coefficients in the single top processes are given in [12].

At NNLO the soft and collinear gluon corrections are

$$\hat{\sigma}^{(2)} = F^{\text{B}} \frac{\alpha_s^2(\mu_{\text{R}}^2)}{\pi^2} \left\{ \frac{1}{2} c_3^2 \left[\frac{\ln^3(1-z)}{1-z} \right]_+ + \dots + \frac{1}{2} c_3^2 c_3^c \ln^3(1-z) + \dots \right\}, \quad (2.4)$$

where we show explicitly only the leading logarithms.

Finally, the NNNLO soft and collinear gluon corrections are

$$\hat{\sigma}^{(3)} = F^{\text{B}} \frac{\alpha_s^3(\mu_{\text{R}}^2)}{\pi^3} \left\{ \frac{1}{8} c_3^3 \left[\frac{\ln^5(1-z)}{1-z} \right]_+ + \dots + \frac{1}{8} c_3^2 c_3^c \ln^5(1-z) + \dots \right\}, \quad (2.5)$$

where again we only show the leading logarithms. Further details are provided in Refs. [12, 14].

3. Single top quark production

The leading-order (LO) diagrams for the production of single top quarks in the t -channel, $qb \rightarrow q't$ and $\bar{q}b \rightarrow \bar{q}'t$; s -channel, $q\bar{q}' \rightarrow \bar{b}t$; and via associated tW production, $bg \rightarrow tW^-$, are shown in Fig. 1.

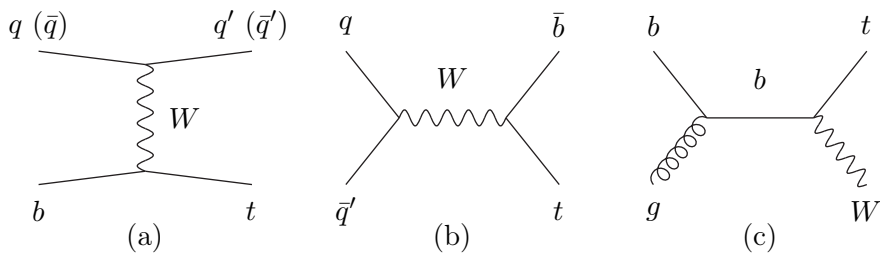


Fig. 1. Leading-order t -channel (a), s -channel (b), and associated tW production (c) diagrams for single top quark production.

Next-to-leading logarithm (NLL) resummation requires that we calculate one-loop corrections in the eikonal approximation to these diagrams. The diagrams for these corrections in the s -channel are shown in Fig. 2. Similar diagrams are used for the t -channel and tW production [12].

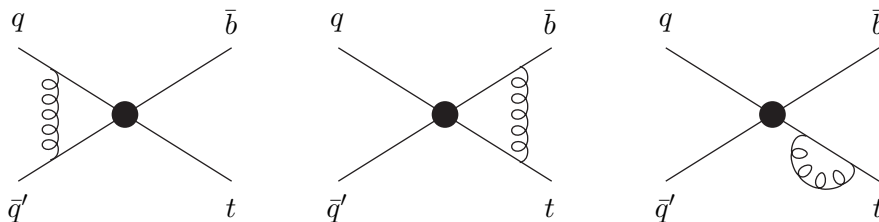


Fig. 2. One-loop eikonal corrections to the soft function for the s -channel diagram in single top quark production.

We now turn our attention to a numerical study of the cross-sections for single-top production at the Tevatron and the LHC [12]. We use the MRST 2004 parton densities [17] in our results.

3.1. Single top production at the Tevatron

We provide below results for single top production at the Tevatron with $\sqrt{S} = 1.96$ TeV, and note that the cross-section for single antitop production is identical to that for the top.

We begin with the t -channel. The soft-gluon corrections in this channel are relatively small. To find the best estimate for the cross-section we match to the exact NLO cross-section, *i.e.* we add the soft-gluon corrections through NNNLO at NLL accuracy [12] to the exact NLO cross-section [18]. The matched cross-section for a top quark mass of 170 GeV is

$$\sigma^{t\text{-channel}}(m_t = 170 \text{ GeV}) = 1.17_{-0.01}^{+0.02} \pm 0.06 \text{ pb}, \quad (3.1)$$

where the first uncertainty is due to the scale dependence, derived by varying the scale between $m_t/2$ and $2m_t$, and the second is due to the parton density uncertainties. The corresponding quantity for a top quark mass of 175 GeV is $1.08_{-0.01}^{+0.02} \pm 0.06$ pb.

Fig. 3 shows the results for the cross-section in the t -channel. On the left we show the LO cross-section as well as the cross-sections with the NLO, NNLO, and NNNLO soft-gluon corrections included versus the top quark mass m_t , with the factorization and renormalization scales set equal to m_t . On the right we plot the scale dependence of the cross-section with $m_t = 175$ GeV. Here we set the factorization scale equal to the renormalization scale and vary this scale μ over a large range.

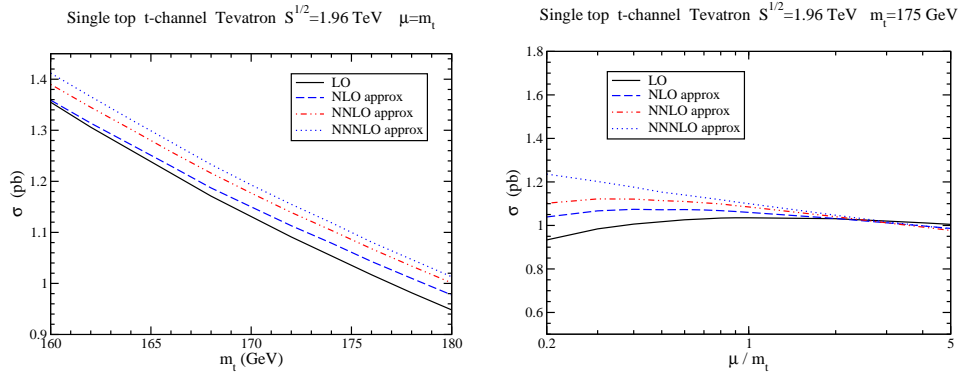


Fig. 3. The cross-section for single top production in the t -channel at the Tevatron.

We continue with the s -channel. The soft-gluon corrections approximate the full QCD corrections very well. The corrections are relatively large for this channel, in stark contrast with the results we found in the t -channel. The matched cross-section (exact NLO + soft gluon corrections through NNNLO) is

$$\sigma^{s\text{-channel}}(m_t = 170 \text{ GeV}) = 0.56 \pm 0.02 \pm 0.01 \text{ pb}, \quad (3.2)$$

while for $m_t = 175$ GeV it is $0.49 \pm 0.02 \pm 0.01$ pb.

In Fig. 4 we plot the cross-section for single top quark production at the Tevatron in the s -channel as a function of m_t setting the scales to $\mu = m_t$. On the left we plot the LO cross-section and the approximate NLO, NNLO, and NNNLO cross-sections at NLL accuracy. The K factors are quite large and are shown on the right.

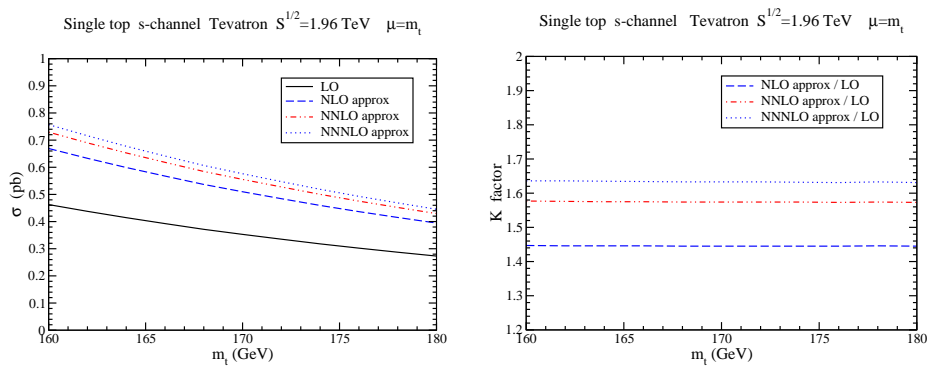


Fig. 4. The cross-section (left) and K factors (right) for single top production in the s -channel at the Tevatron.

The cross-section for single top production at the Tevatron via the tW -channel is numerically the smallest. The approximate NNNLO cross-section is

$$\sigma^{tW}(m_t = 170 \text{ GeV}) = 0.15 \pm 0.02 \pm 0.03 \text{ pb} \quad (3.3)$$

and it is $0.13 \pm 0.02 \pm 0.02$ pb for $m_t = 175$ GeV.

3.2. Single top production at the LHC

We now show results for single top production at the LHC with $\sqrt{S} = 14$ TeV. At the LHC the top and antitop cross-sections are different in the t - and s -channels.

In the t -channel the threshold corrections are not a good approximation of the full QCD corrections. The exact NLO cross-section is $152 \pm 5 \pm 3$ pb for $m_t = 170$ GeV, and $146 \pm 4 \pm 3$ pb for $m_t = 175$ GeV. For antitop production in the t -channel the exact NLO cross-section is $93 \pm 3 \pm 2$ pb for $m_t = 170$ GeV, and $89 \pm 3 \pm 2$ pb for $m_t = 175$ GeV.

For single top production at the LHC through the s -channel the matched cross-section, *i.e.* exact NLO plus soft gluon corrections through NNNLO, is

$$\sigma_{\text{top}}^{s\text{-channel}}(m_t = 170 \text{ GeV}) = 8.0_{-0.5}^{+0.6} \pm 0.1 \text{ pb} \quad (3.4)$$

and the corresponding cross-section for $m_t = 175$ GeV is $7.2_{-0.5}^{+0.6} \pm 0.1$ pb.

For single antitop production at the LHC in the s -channel the matched cross-section is

$$\sigma_{\text{antitop}}^{s\text{-channel}}(m_t = 170 \text{ GeV}) = 4.5 \pm 0.1 \pm 0.1 \text{ pb} \quad (3.5)$$

and it is $4.0 \pm 0.1 \pm 0.1$ pb for $m_t = 175$ GeV.

In Fig. 5 we plot the cross-section for single top quark (left) and single antitop quark (right) production at the LHC in the s -channel as a function of m_t setting the scales to $\mu = m_t$.

For the tW -channel, the matched cross-section (exact NLO [19] plus NNNLO soft corrections) is

$$\sigma^{tW}(m_t = 170 \text{ GeV}) = 44 \pm 5 \pm 1 \text{ pb} \quad (3.6)$$

and the result for $m_t = 175$ GeV is $41 \pm 4 \pm 1$ pb. The cross-section for anti-top production in this channel is identical to that for top.

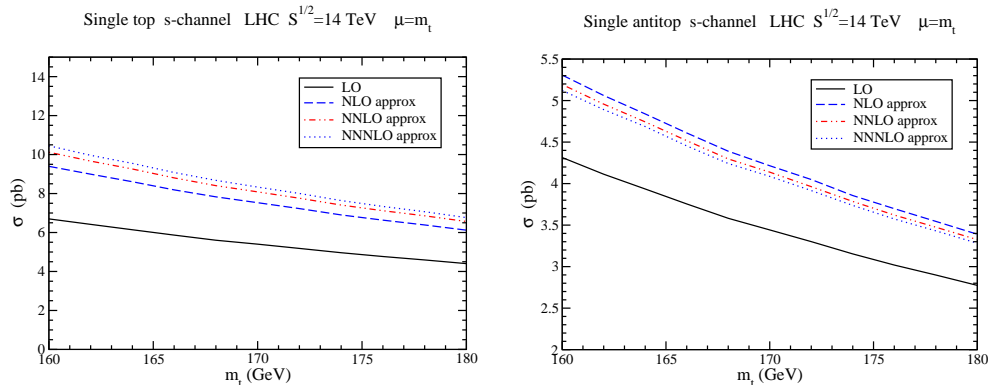


Fig. 5. The cross-section for single top (left) and single antitop (right) production in the s -channel at the LHC.

In Fig. 6 we plot the cross-section (left) and K factors (right) for tW production at the LHC as functions of m_t , setting the scales to $\mu = m_t$. The higher-order corrections are quite significant as shown by the large K factors.

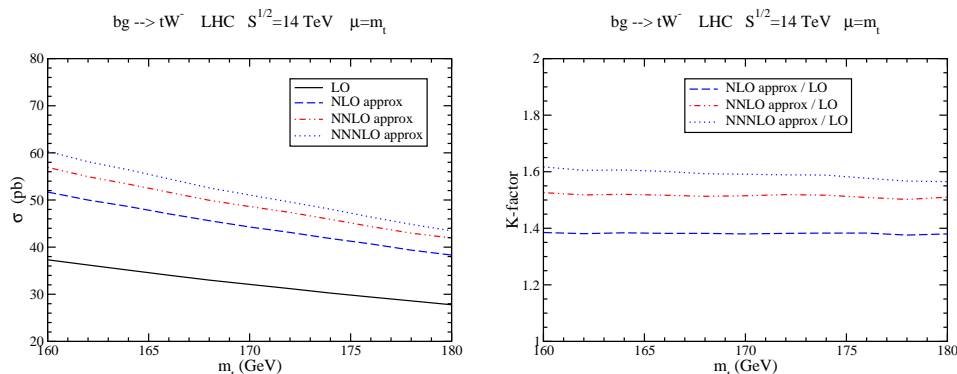


Fig. 6. The cross-section (left) and K factors (right) for tW production at the LHC.

4. Higgs production via $b\bar{b} \rightarrow H$

The process $b\bar{b} \rightarrow H$ has a very simple color structure and kinematics, and is very similar to the Drell–Yan process. The QCD corrections are fully known to NNLO [20]. We can calculate all soft corrections fully to NNNLO [13, 14]. However, it is found that the soft-gluon approximation is inadequate: purely collinear terms must be included to provide a good approximation. The collinear terms can be resummed at LL accuracy, and

good approximations at NLL and NNLL accuracy were provided in [14]. Below we provide numerical results for the cross-section at the Tevatron and the LHC using the MRST 2006 parton densities [21].

In Fig. 7 we show the contribution of various terms to the complete NNLO corrections for Higgs production via $b\bar{b} \rightarrow H$ with $\mu = m_H$ at the Tevatron (left-hand side) and the LHC (right-hand side). In this figure NNLO denotes the $\mathcal{O}(\alpha_s^2)$ corrections only, without the LO term and NLO corrections. The curve marked NNLO S+V / NNLO denotes the percentage contribution of the NNLO soft plus virtual (S+V) corrections to the total NNLO corrections. We see that both at the Tevatron and the LHC this contribution is small. Inclusion of the leading collinear (LC) logarithms accounts for about 60% of the total NNLO corrections at both the Tevatron and the LHC. Including the next-to-leading collinear (NLC) logarithms vastly improves the approximation. The difference between the S+V+LC

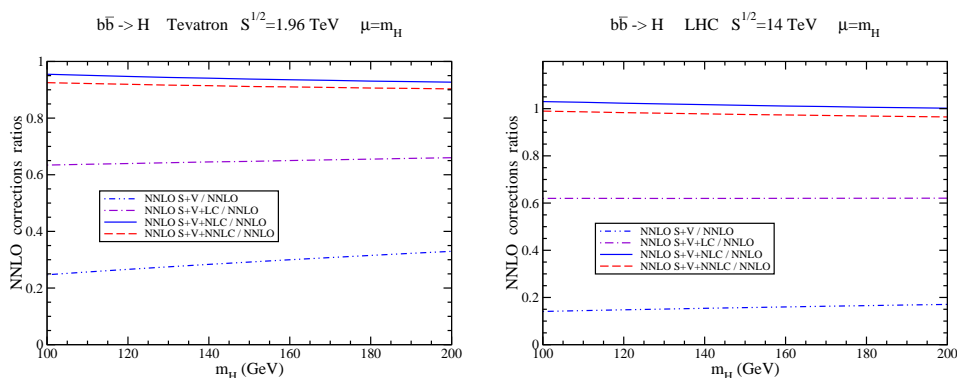


Fig. 7. The NNLO ratios for $b\bar{b} \rightarrow H$ at the Tevatron (left) and the LHC (right). Here $\mu = \mu_F = \mu_R = m_H$.

and the S+V+NLC curves is around 30% at the Tevatron and 40% at the LHC; thus the NLC terms are of great importance in achieving a good approximation. We also plot a curve (S+V+NNLC) that in addition includes the next-to-next-to-leading collinear (NNLC) terms. The NNLC terms alone do not make a large contribution, and the S+V+NNLC results approximate the exact NNLO corrections very well, especially at the LHC.

In Fig. 8 we plot the cross-sections (left) and K factors (right) for $b\bar{b} \rightarrow H$ at the Tevatron with $\mu = m_H$. The complete NLO corrections increase the LO result by over 60%. The NNLO corrections further increase the cross-section by roughly an additional 30%. Finally, we include the soft and purely collinear corrections at NNNLO. The soft corrections are complete and the purely collinear terms are approximate. Our study of the contributions of the soft and collinear terms at NNLO gives us confidence that the NNNLO

S+NNLCapp curves provide a good approximation of the complete NNNLO cross-section. The NNNLO S+NNLCapp corrections provide an additional 10% to 15% increase to the cross-section.

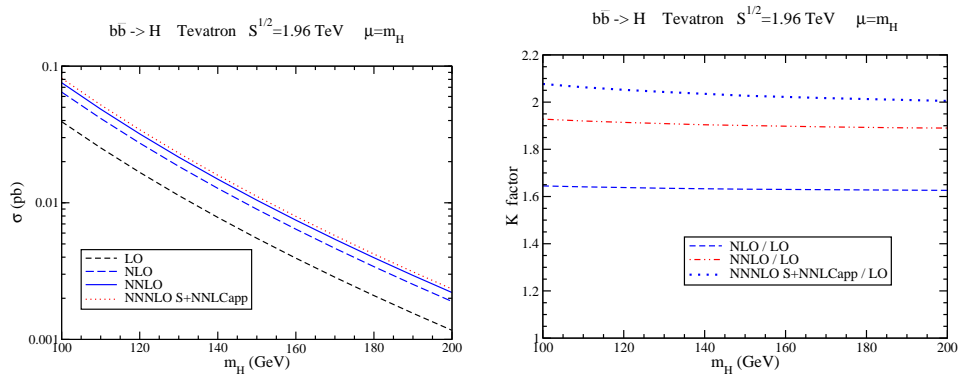


Fig. 8. The cross-section (left) and K factors (right) for $b\bar{b} \rightarrow H$ at the Tevatron. Here $\mu = \mu_F = \mu_R = m_H$.

In Fig. 9 we plot the cross-sections (left) and K factors (right) for $b\bar{b} \rightarrow H$ at the LHC for $\mu = m_H$. We see that the K factors here are quite similar (slightly smaller) to those for the Tevatron.

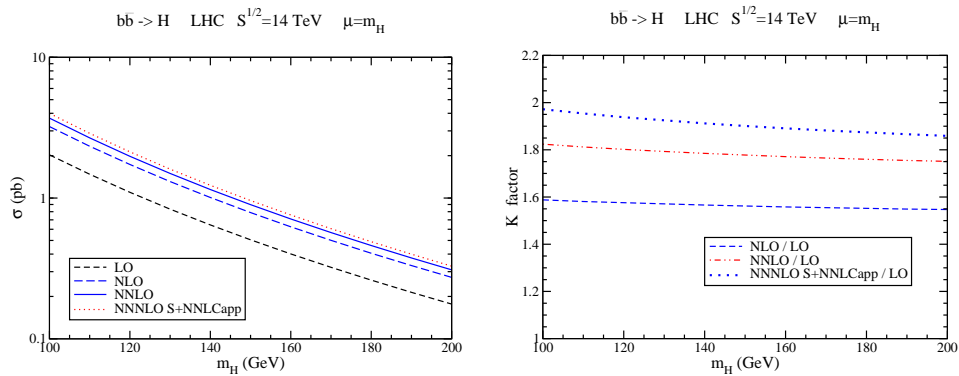


Fig. 9. The cross-section (left) and K factors (right) for $b\bar{b} \rightarrow H$ at the LHC. Here $\mu = \mu_F = \mu_R = m_H$.

Finally, we note that the parton distribution function uncertainties for this process are non-negligible and can be of the same order of magnitude as the scale uncertainty, especially for large Higgs masses at the Tevatron.

5. Conclusion

The soft and collinear corrections make important contributions in the cross-sections for single top quark production and for Higgs boson production at the Tevatron and the LHC. From the resummation formalism we have derived NNNLO expansions which we use to calculate these corrections.

For single top quark production the soft approximation works well for all channels at the Tevatron, and for the s -channel and tW production at the LHC. The soft-gluon corrections are quite significant.

For Higgs production via the process $b\bar{b} \rightarrow H$ we also have to include purely collinear terms. The collinear+soft approximation is excellent and the corrections through NNNLO are considerable.

This work was supported by the National Science Foundation under the grant No. PHY 0555372.

REFERENCES

- [1] [CDF Collaboration], *Phys. Rev. Lett.* **74**, 2626 (1995) [[hep-ex/9503002](#)].
- [2] [D0 Collaboration], *Phys. Rev. Lett.* **74**, 2632 (1995) [[hep-ex/9503003](#)].
- [3] W. Wagner, *Rept. Prog. Phys.* **68**, 2409 (2005) [[hep-ph/0507207](#)].
- [4] R. Kehoe, M. Narain, A. Kumar, *Int. J. Mod. Phys.* **A23**, 353 (2008) [[arXiv:0712.2733\[hep-ex\]](#)].
- [5] N. Kidonakis, R. Vogt, *Phys. Rev.* **D68**, 114014 (2003) [[hep-ph/0308222](#)].
- [6] [CDF Collaboration], *Phys. Rev. Lett.* **96**, 202002 (2006) [[hep-ex/0603043](#)]; *Phys. Rev.* **D74**, 072006 (2006) [[hep-ex/0607035](#)]; *Phys. Rev.* **D74**, 072005 (2006) [[hep-ex/0607095](#)]; *Phys. Rev.* **D76**, 072009 (2007) [[arXiv:0706.3790\[hep-ex\]](#)].
- [7] [D0 Collaboration], *Phys. Rev.* **D74**, 112004 (2006) [[hep-ex/0611002](#)]; *Phys. Rev.* **D76**, 072007 (2007) [[hep-ex/0612040](#)]; *Phys. Rev.* **D76**, 092007 (2007) [[arXiv:0705.2788\[hep-ex\]](#)]; *Phys. Rev.* **D76**, 052006 (2007) [[arXiv:0706.0458\[hep-ex\]](#)].
- [8] [D0 Collaboration], *Phys. Rev. Lett.* **98**, 181802 (2007) [[hep-ex/0612052](#)].
- [9] [CDF Collaboration], Conf. Note 8964; Conf. Note 8968.
- [10] P.W. Higgs, *Phys. Rev. Lett* **12**, 132 (1964); *Phys. Rev. Lett.* **13**, 508 (1964); *Phys. Rev.* **145**, 1156 (1966); F. Englert, R. Brout, *Phys. Rev. Lett.* **13**, 321 (1964); G.S. Guralnik, C.R. Hagen, T.W.B. Kibble, *Phys. Rev. Lett.* **13**, 585 (1964).
- [11] [Higgs Working Group], Summary Report, Les Houches Workshop: Physics at TeV Colliders, Les Houches, France, 26 May–6 Jun 2003, p. 1 [[hep-ph/0406152](#)], and references therein.

- [12] N. Kidonakis, *Phys. Rev.* **D74**, 114012 (2006) [[hep-ph/0609287](#)]; *Phys. Rev.* **D75**, 071501(R) (2007) [[hep-ph/0701080](#)]; DIS2007, p. 443, [arXiv:0705.2431](#) [[hep-ph](#)].
- [13] V. Ravindran, *Nucl. Phys.* **B752**, 173 (2006) [[hep-ph/0603041](#)].
- [14] N. Kidonakis, *Phys. Rev.* **D77**, 053008 (2008) [[arXiv:0711.0142](#) [[hep-ph](#)]].
- [15] N. Kidonakis, *Int. J. Mod. Phys.* **A19**, 1793 (2004) [[hep-ph/0303186](#)]; *Mod. Phys. Lett.* **A19**, 405 (2004) [[hep-ph/0401147](#)]; DIS2003, p. 429, [hep-ph/0307207](#); DIS2003, p. 465, [hep-ph/0306125](#); DPF2004, *Int. J. Mod. Phys.* **A20**, 3726 (2005) [[hep-ph/0410116](#)].
- [16] N. Kidonakis, *Phys. Rev.* **D73**, 034001 (2006) [[hep-ph/0509079](#)]; *PoS HEP2005*, 055 (2006) [[hep-ph/0512017](#)]; DIS 2006, p. 463, [hep-ph/0606280](#).
- [17] A.D. Martin, R.G. Roberts, W.J. Stirling, R.S. Thorne, *Phys. Lett.* **B604**, 61 (2004) [[hep-ph/0410230](#)].
- [18] B.W. Harris, E. Laenen, L. Phaf, Z. Sullivan, S. Weinzierl, *Phys. Rev.* **D66**, 054024 (2002) [[hep-ph/0207055](#)].
- [19] S.H. Zhu, *Phys. Lett.* **B524**, 283 (2002) [[hep-ph/0109269](#)]; *Phys. Lett.* **B537**, 351 (2002).
- [20] R.V. Harlander, W.B. Kilgore, *Phys. Rev.* **D68**, 013001 (2003) [[hep-ph/0304035](#)].
- [21] A.D. Martin, W.J. Stirling, R.S. Thorne, G. Watt, *Phys. Lett.* **B652**, 292 (2007) [[arXiv:0706.0459](#)].